

Capillary plugs in horizontal rectangular tubes with non-uniform contact angles

Chengwei Zhu^{1,2}, Xinping Zhou^{1,†} and Gang Zhang^{1,2}

¹School of Mechanical Science and Engineering, Huazhong University of Science and Technology, Wuhan 430074, PR China

²Department of Mechanics, Huazhong University of Science and Technology, Wuhan 430074, PR China

(Received 28 December 2019; revised 6 July 2020; accepted 18 July 2020)

The aim of this paper is to make the formation of liquid plugs as difficult as possible in liquid partially filling a horizontal rectangular tube in a downward gravity field by setting the walls to have differing contact angles. Manning *et al.*'s method (*J. Fluid Mech.*, vol. 682, 2011, pp. 397–414), extended from Concus–Finn theory, is applied to the existence of capillary plugs in rectangular tubes. The critical Bond numbers (B_c) determining the existence of capillary plugs in a rectangular tube are studied for different settings of the non-uniform contact angles, and the influence of the aspect ratio (defined as the width-to-height ratio) of the rectangular cross-section on B_c is examined. Compared to the maximum and minimum of B_c reached for uniform contact angles, the maximum of B_c is higher, which is attained for the bottom contact angle $\gamma_2 = 135^\circ$, the top contact angle $\gamma_4 = 45^\circ$, and the side contact angles $\gamma_1 = \gamma_3 = 90^\circ$; while the minimum is considerably lowered to zero, which is reached for $\gamma_1 = \gamma_2 = 45^\circ$ and $\gamma_3 = \gamma_4 = 135^\circ$. The aspect ratio of the rectangle has no influence on the maximum and minimum B_c for a tube with walls of differing contact angles. There is only one non-occluded liquid topology in a square, while two topologies may occur in a rectangle with aspect ratio 2, and the transition between the two topologies is accompanied by a kink of the curve of B_c . Optimization of the non-uniform contact angles can facilitate or effectively block the capillary plugs in rectangular tubes regardless of the aspect ratios.

Key words: capillary flows

1. Introduction

A liquid plug in a container with a small cross-section may or may not occur depending on the container geometry, gravity and surface tension. An understanding of the hydrostatics of liquid plugs in a container is important in a number of applications.

[†] Email address for correspondence: xpzhou08@hust.edu.cn

Examples include liquid plugs in fuel cells (Herescu & Allen 2012), liquid filling in a gap in micro-gravity (Chen & Collicott 2006), and liquid occlusion in microfluidics and micro-electromechanical systems (Gravesen, Branebjerg & Jensen 1993). Liquid plugs may be harmful to the performance of the equipment. Generally, it is very important to optimally design the containers (mainly including designing the tube geometry and setting the material surface properties) to avoid liquid plugs in them.

To understand the liquid plug phenomenon, it is necessary to find the equilibrium capillary surfaces spanning the containers and to propose criteria for the occlusion of the liquid. Concus & Finn (1969) and Finn (1986) developed a well-known theory to propose criteria for the existence and non-existence of an occluding capillary surface in a cylinder for cases under weightless conditions or in a gravity field parallel to the axis of the cylinder. Smedley (1990) applied Finn's (1986) theory to the cases of four different cross-sections (one of them being eccentric annuli) for various wetting angles under weightless conditions. Pour & Thiessen (2019) extended Smedley's (1990) work to the case of both non-wetting and wetting liquids with a given sufficient volume in an annular geometry between two non-concentric cylinders under weightless conditions. In a geometric parameter space, they found the occluding region where only the occluding configuration occurs, the non-occluding region where only the non-occluding bridging configuration occurs, and a bistable region where either configuration can exist.

De Lazzer *et al.* (1996) used a numerical method to calculate the capillary pressure in a rotating polygonal cylinder, when a body force is perpendicular to the axis of the cylinder. De Lazzer *et al.* (2003) investigated the shapes of liquids pinned between two parallel plates under the effect of a lateral body force. Manning, Collicott & Finn (2011) extended the known theory (Concus & Finn 1969; Finn 1986) to include transverse body forces, leading to an explicit mathematically rigorous occlusion criterion for cylindrical tubes in a transverse body force field, depending on the force magnitude and contact angle. The critical Bond number was used as an important parameter to determine the existence or non-existence of capillary plugs. If the Bond number is less than the critical Bond number, a plug in the tube may occur; otherwise a plug in the tube will not occur. They presented a precise analytic criterion for a liquid plug in a circular cylinder. Manning *et al.*'s (2011) analytic theory is in good agreement with direct calculations for the surfaces of minimizing energy via Surface Evolver (Brakke 1992) in three-dimensional mode. Based on the Manning *et al.* (2011) theory, Manning & Collicott (2015) presented an exhaustive determination of the critical Bond number for the existence of occluding capillary surfaces in horizontal rectangular channels with uniform contact angles in a downward gravity field. The effects of aspect ratios (defined as the width-to-height ratio) and contact angles on the critical Bond number of the rectangular tube were examined. The critical Bond numbers for liquid plugs in the tubes with different cross-sectional shapes (including circle, oblate and prolate ellipses of different aspect ratios, and triangles) and different contact angles were determined (Rascón, Parry & Aarts 2016).

Researchers have sought to find methods for preventing the existence of liquid plugs. For this purpose, a wedge was found by Concus & Finn (1969) to be able to avoid liquid plugs in a cylindrical container. When the sum of the contact angle and half of the interior angle of the corner is less than 90° , a liquid plug will not occur or the surface will not exist. Manning *et al.* (2011) designed a 'flattened ice-cream cone' cylinder in which non-occluding will occur. Square hydrophilic channels are utilized in fuel cells to prevent liquid water plugs in them (Zhang, Yang & Wang 2006). Compared to the contact angle $\gamma = 90^\circ$, both $\gamma > 90^\circ$ and $\gamma < 90^\circ$ can decrease the critical Bond number (Manning

et al. 2011). A sufficiently large aspect ratio can lead to reduction of the critical Bond number of a rectangular tube (Manning & Collicott 2015). However, in some applications, the cross-section of the liquid partially filling the tube is determined mainly by the performance of the equipment containing the flow tube and may not be changed only due to the liquid plug performance. Furthermore, the reduction of critical Bond number due to $\gamma > 90^\circ$ or $\gamma < 90^\circ$ and the use of rectangular cross-section of very large aspect ratio (Manning & Collicott 2015) is small, and the value of the critical Bond number is of the same order of magnitude as before. It is necessary to seek alternative methods of making the formation of liquid plugs as difficult as possible.

The above work has been focused on finding the equilibrium capillary surfaces and determining the critical Bond numbers for liquid plugs in tubes, where the contact angles on the walls are uniform. What are the configurations of the equilibrium capillary surfaces in infinitely long tubes with walls of differing contact angles (called non-uniform contact angles here)? How does the non-uniformity of contact angles influence the critical Bond numbers for liquid plugs in the tubes? Is the non-uniformity of contact angles helpful for obtaining much smaller critical Bond numbers or not? These questions have not been studied to date. Here, we answer them by taking rectangular tubes as an example, because a rectangle can serve as a canonical form to extend to other polygonal shapes.

In this paper, a mathematical model that considers the effects of transverse gravity and surface tension is given to calculate equilibrium capillary surfaces in infinitely long rectangular tubes. Manning *et al.*'s (2011) method is applied to the existence of capillary plugs in rectangular tubes. The effect of different settings of the non-uniform contact angles on the critical Bond number is investigated. Finally, the critical Bond numbers for liquid plugs in the rectangular tubes with the walls of differing contact angles for different aspect ratios are determined.

2. Methods

Consider a long horizontal rectangular tube partially filled with a liquid in a downward gravity field, as depicted in [figure 1](#). The length of the tube is assumed infinite; w and h are the width and height of the tube cross-section, respectively; and the aspect ratio is defined as w/h . The gas and the liquid in the tube are immiscible fluids and both of them have very large fixed volumes. Physically, the static equilibrium of the gas–liquid interface is supported by gravity and the surface tension forces at contact points (contact lines in three dimensions).

2.1. Young–Laplace equation in two dimensions

We assume that the gas–liquid interface is in equilibrium in a horizontal rectangular tube in a downward gravity field ([figure 1](#)). By solving the Young–Laplace equation in two dimensions (Bhatnagar & Finn 2016):

$$\left(\frac{y_x}{\sqrt{1 + y_x^2}} \right)_x \equiv (\sin \psi)_x = \lambda + \kappa y, \quad (2.1)$$

the height $y(x)$ of the liquid surface can be determined, yielding the equilibrium condition for the gas–liquid interface. In this equation, the subscript x represents the derivative with respect to the coordinate x (i.e. $(\cdot)_x \equiv d(\cdot)/dx$), ψ is the inclination angle of the curve $y(x)$ and $\kappa = \rho g/\sigma$ is the capillary constant, with ρ the density difference (positive) between

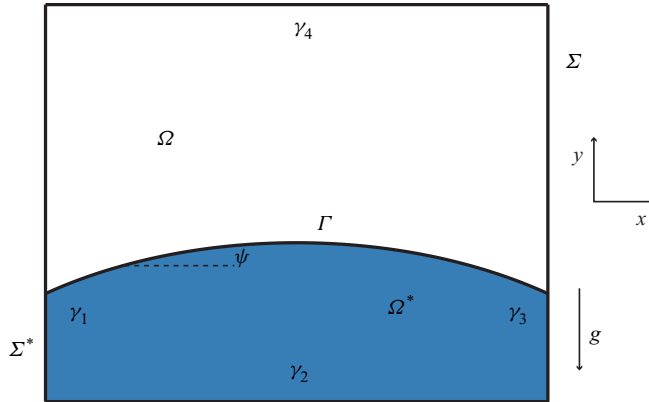


FIGURE 1. Schematic of general cross-section of liquid partially filling a rectangular tube in a downward gravity field. The interior Ω is divided into Ω^* and $(\Omega - \Omega^*)$ by the arc Γ ; the perimeter Σ is divided into Σ^* and $(\Sigma - \Sigma^*)$; ψ is the inclination angle on the arc Γ ; and γ_1 , γ_2 , γ_3 and γ_4 are the contact angles of the four walls, respectively.

liquid and gas, g the gravitational acceleration, σ the surface tension of the interface, and λ is a constant depending on the eventual volume constraint. The boundary condition remains as

$$\mathbf{v} \cdot \mathbf{T}\mathbf{y} = \cos \gamma, \quad \mathbf{T}\mathbf{y} \equiv \nabla y / \sqrt{1 + |\nabla y|^2}, \quad (2.2)$$

where \mathbf{v} is the unit exterior normal to the rectangle on Σ , and γ is the contact angle.

We can obtain the solutions of (2.1) by integrating the parametrization form of (2.1). There are two parametrization forms of (2.1). Following Bhatnagar & Finn (2016), we have

$$\frac{dx}{d\psi} = \frac{\cos \psi}{\lambda + \kappa y}, \quad \frac{dy}{d\psi} = \frac{\sin \psi}{\lambda + \kappa y}. \quad (2.3a,b)$$

A first integral of the form is (Bhatnagar & Finn 2016; Zhou & Zhang 2017):

$$c = \frac{(\lambda + \kappa y_0)^2}{2\kappa} + \cos \psi_0. \quad (2.4)$$

The solutions according to the range of the integral constant c are uniquely determined by the prescribed point (x_0, y_0) on the interface and the inclination angle ψ_0 of the interface at the prescribed point. Explicitly integrating the terms of (2.3a,b), we obtain

$$x = x_0 + \int_{\psi_0}^{\psi} \frac{\cos \tau}{\pm \sqrt{2\kappa(c - \cos \tau)}} d\tau, \quad \psi \in \left[\psi_0, \frac{\pi}{2} \right], \quad (2.5)$$

$$y = -\frac{\lambda}{\kappa} \pm \frac{1}{\kappa} \sqrt{2\kappa(c - \cos \psi)}. \quad (2.6)$$

Equation (2.1) also can be parametrized by the arclength s (Finn 1986) as

$$\frac{dx}{ds} = \cos \psi, \quad \frac{dy}{ds} = \sin \psi, \quad \frac{d\psi}{ds} = \frac{dx}{ds} \frac{d\psi}{dx} = \lambda + \kappa y, \quad (2.7a-c)$$

which hold the solution curves (corresponding to $0 < c < 1$ in (2.4)–(2.6)) each containing an inflection point. Equations (2.5) and (2.6) are employed in calculation for

the family of solution curves with $c > 1$, and (2.7a–c) are employed in calculation for the family of solution curves with $0 < c \leq 1$.

2.2. Occlusion criteria

The plug criterion for an infinitely long horizontal rectangular tube partially filled by liquid in a downward gravity field is developed by extending Manning *et al.*'s (2011) plug criterion for a cylindrical tube. The two inequalities that are necessary for the existence of an occluding interface are

$$\Phi[\Omega^*] \equiv |\Gamma| - \int_{\Sigma^*} \cos \gamma + \frac{|\Omega^*|}{|\Omega|} \int_{\Sigma} \cos \gamma + \kappa \int_{\Omega^*} y > 0, \quad (2.8)$$

and

$$\Psi[\Omega^*] \equiv |\Gamma| + \int_{\Sigma^*} \cos \gamma - \frac{|\Omega^*|}{|\Omega|} \int_{\Sigma} \cos \gamma - \kappa \int_{\Omega^*} y > 0. \quad (2.9)$$

If one of the above two inequalities is not satisfied for an Ω^* , a plug surface will not exist. We choose the constant λ as

$$\lambda = \frac{1}{|\Omega|} \int_{\Sigma} \cos \gamma = \frac{(\cos \gamma_1 + \cos \gamma_3) + (w/h)(\cos \gamma_2 + \cos \gamma_4)}{w}, \quad (2.10)$$

and the centroid of the rectangle lies on the x -axis. The Bond number (B) is defined based on the height of the tube cross-section h (used as the characteristic length) as $B = (\rho g/\sigma)h^2$. The critical Bond number (B_c) is used as the parameter to determine the existence or non-existence of capillary plugs. If $B < B_c$, a plug in the tube may occur; otherwise, a plug will not occur. Newton's method is used for iterative computations of the above equations.

3. Results and discussion

3.1. Effect of uniform contact angles

For contact angles smaller than 45° or larger than 135° , the liquid will critically wet the corners of the rectangle regardless of the Bond number (Concus & Finn 1969). The critical Bond numbers of a square tube and a rectangular tube of $w/h = 2$ for uniform contact angles ($\gamma_1 = \gamma_2 = \gamma_3 = \gamma_4$) varying from 45° to 135° with an increment of 1° are shown in figure 2. The results are in excellent agreement with those calculated by Manning & Collicott (2015). The curve is symmetric about the vertical line $\gamma = 90^\circ$ (verified in § 3.2) and reaches a maximum at $\gamma = 90^\circ$. In other words, both $\gamma > 90^\circ$ and $\gamma < 90^\circ$ can lead to the reduction of B_c . The contact angle γ can be found to produce the same B_c value as the contact angle $180^\circ - \gamma$. Furthermore, different from the smooth curve of the square, the curve for $w/h = 2$ has two kinks (each corresponding to a topological change in the non-occluded liquid configuration between a single connected region and two separated corner regions) at $\gamma = 49^\circ$ and 131° so that the minimum of B_c is smaller than that of the square tube (also see Manning & Collicott 2015).

3.2. Effect of non-uniform contact angles

In reality, the contact angle on one wall of a tube may be different from the contact angles on the other walls. We take a square tube as an example to analyse the effect of

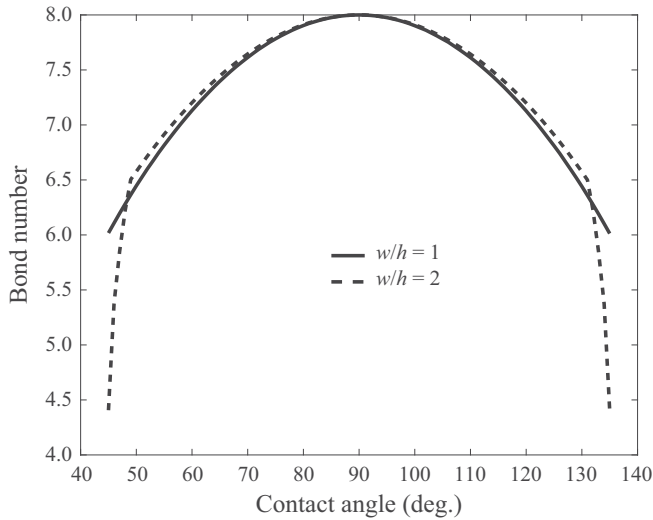


FIGURE 2. Critical Bond numbers of two rectangular tubes versus uniform contact angles.

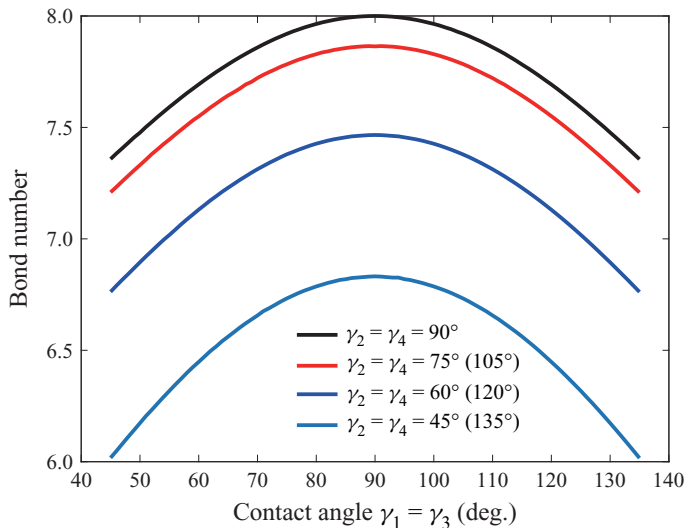


FIGURE 3. Critical Bond number of a square tube for different values of contact angles $\gamma_2 = \gamma_4$ versus contact angles $\gamma_1 = \gamma_3$.

the non-uniform contact angles on B_c . Owing to the symmetry of the two sidewalls, the effect of the contact angle of one sidewall γ_1 is equivalent to the effect of the contact angle of the other sidewall γ_3 . Figure 3 shows the variations of B_c for different contact angles ($\gamma_2 = \gamma_4 = 45^\circ, 60^\circ, 75^\circ, 90^\circ, 105^\circ, 120^\circ$ and 135°) with the contact angles $\gamma_1 = \gamma_3$. In figure 3, the curves are still symmetric about the vertical line $\gamma_1 = \gamma_3 = 90^\circ$ and reach maxima at $\gamma_1 = \gamma_3 = 90^\circ$. A larger difference in the contact angles $\gamma_2 = \gamma_4$ from 90° leads to the reduction of B_c . However, the maximum and minimum of B_c do not change any more compared to the case for the uniform contact angles ($\gamma_1 = \gamma_2 = \gamma_3 = \gamma_4$).

In order to further analyse the effect of the non-uniformity of γ_2 and γ_4 effectively, the contact angles studied have the relationship $\gamma_4 = 180^\circ - \gamma_2$. In this case, the maximum

Plugs in horizontal tubes with non-uniform contact angles

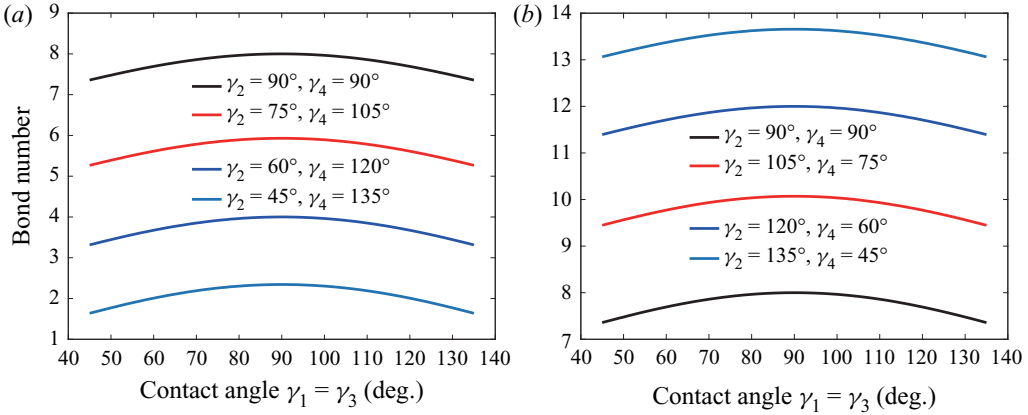


FIGURE 4. Critical Bond number of a square tube for different values of contact angles γ_2 and $\gamma_4 = 180^\circ - \gamma_2$ versus contact angles $\gamma_1 = \gamma_3$.

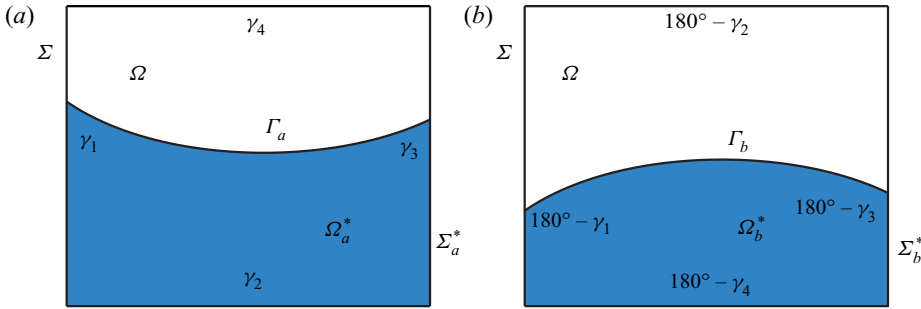


FIGURE 5. Interface of rectangular tube (a) with contact angles $\gamma_1, \gamma_2, \gamma_3$ and γ_4 and (b) with $\gamma_1^+ = 180^\circ - \gamma_1, \gamma_2^+ = 180^\circ - \gamma_2, \gamma_3^+ = 180^\circ - \gamma_3$ and $\gamma_4^+ = 180^\circ - \gamma_4$.

non-uniformity of the two contact angles is generated when $\gamma_2 = 45^\circ$ or 135° . It is found from figure 4 that the lower contact angle on the bottom wall with the greater contact angle on the top wall can lead to effective reduction of B_c , and, in contrast, the reverse can lead to effective increase of B_c . The minimum is reached for $\gamma_2 = 45^\circ$ and $\gamma_4 = 135^\circ$ and the maximum of 13.66 is attained for $\gamma_2 = 135^\circ$ and $\gamma_4 = 45^\circ$.

We will analyse the effect of the non-uniformity of the two side contact angles γ_1 and γ_3 based on the maximum non-uniformity of the bottom and top contact angles. In order to reduce the number of representative cases for comprehensive study in this respect as much as possible, we initially analyse the relationship of B_c for the case with contact angles $\gamma_1, \gamma_2, \gamma_3$ and γ_4 and that for the case with $\gamma_1^+ = 180^\circ - \gamma_1, \gamma_2^+ = 180^\circ - \gamma_2, \gamma_3^+ = 180^\circ - \gamma_3$ and $\gamma_4^+ = 180^\circ - \gamma_4$. The interfaces of the two cases are shown in figure 5. Since (2.8) and (2.9) are equivalent, we compare the values of Φ for the two cases. For the two cases as shown in figures 5(a) and 5(b) the Φ values are, respectively,

$$\begin{aligned} \Phi_a = & |\Gamma_a| - (|\Sigma_{a1}^*| \cos \gamma_1 + |\Sigma_{a2}^*| \cos \gamma_2 + |\Sigma_{a3}^*| \cos \gamma_3 + |\Sigma_{a4}^*| \cos \gamma_4) \\ & + \frac{|\Omega_a^*|}{|\Omega|} \int_{\Sigma} \cos \gamma + \kappa \int_{\Omega_a^*} y, \end{aligned} \quad (3.1)$$

and

$$\begin{aligned} \Phi_b = & |\Gamma_b| - (|\Sigma_{b1}^*| \cos \gamma_1^+ + |\Sigma_{b2}^*| \cos \gamma_2^+ + |\Sigma_{b3}^*| \cos \gamma_3^+ + |\Sigma_{b4}^*| \cos \gamma_4^+) \\ & + \frac{|\Omega_b^*|}{|\Omega|} \int_{\Sigma} \cos \gamma^+ + \kappa \int_{\Omega_b^*} y. \end{aligned} \tag{3.2}$$

From (2.5), (2.6) and (2.10), we find that the y values of the two interfaces are symmetric about the x -axis. Therefore, $\kappa \int_{\Omega_b^*} y = \kappa \int_{\Omega_a^*} y$. Moreover, the arlengths, the areas and the perimeters have the relations, respectively: $|\Gamma_a| = |\Gamma_b|$, $|\Omega_a^*| = |\Omega| - |\Omega_b^*|$ and $|\Sigma_a^*| = |\Sigma| - |\Sigma_b^*|$. In this case, (3.2) can be rewritten as

$$\begin{aligned} \Phi_b = & |\Gamma_a| - \left(\int_{\Sigma} \cos \gamma^+ - |\Sigma_{a1}^*| \cos \gamma_1^+ - |\Sigma_{a2}^*| \cos \gamma_4^+ - |\Sigma_{a3}^*| \cos \gamma_3^+ \right. \\ & \left. - |\Sigma_{a4}^*| \cos \gamma_2^+ \right) + \frac{(|\Omega| - |\Omega_a^*|)}{|\Omega|} \int_{\Sigma} \cos \gamma^+ + \kappa \int_{|\Omega_a^*|} y \\ = & |\Gamma_a| + (|\Sigma_{a1}^*| \cos \gamma_1^+ + |\Sigma_{a2}^*| \cos \gamma_4^+ + |\Sigma_{a3}^*| \cos \gamma_3^+ + |\Sigma_{a4}^*| \cos \gamma_2^+) \\ & - \frac{|\Omega_a^*|}{|\Omega|} \int_{\Sigma} \cos \gamma^+ + \kappa \int_{|\Omega_a^*|} y. \end{aligned} \tag{3.3}$$

Based on the relation of the contact angles as shown in figure 5(a) and those in figure 5(b), $\int_{\Sigma} \cos \gamma^+$ is equal to $-\int_{\Sigma} \cos \gamma$ from (2.10), and Φ_b is equal to Φ_a from (3.1) and (3.3). It is concluded that the value of B_c of a rectangular tube with contact angles $\gamma_1, \gamma_2, \gamma_3$ and γ_4 is equal to that with $\gamma_1^+ = 180^\circ - \gamma_1, \gamma_2^+ = 180^\circ - \gamma_4, \gamma_3^+ = 180^\circ - \gamma_3$ and $\gamma_4^+ = 180^\circ - \gamma_2$. (The uniform contact angles of $\gamma_1 = \gamma_2 = \gamma_3 = \gamma_4 = \gamma$, and $\gamma_1^+ = \gamma_2^+ = \gamma_3^+ = \gamma_4^+ = 180^\circ - \gamma$ are special cases. The B_c value for the uniform contact angle γ is equal to that for the uniform contact angle $180^\circ - \gamma$.) In this case, the range of γ_1 from 45° to 135° and the range of γ_3 from 90° to 135° are representative for the comprehensive studies on the influence of the non-uniformity of γ_1 and γ_3 .

The critical Bond numbers of a square tube versus contact angle γ_1 with γ_3 changing among $90^\circ, 105^\circ, 120^\circ$ and 135° for the case $\gamma_2 = 45^\circ$ and $\gamma_4 = 135^\circ$ and the case $\gamma_2 = 135^\circ$ and $\gamma_4 = 45^\circ$ are shown in figure 6. The curve is no longer symmetric about the vertical line of 90° , as it is in figures 2–4. The minimum of $B_c = 0$ reached at $\gamma_1 = \gamma_2 = 45^\circ$ and $\gamma_3 = \gamma_4 = 135^\circ$ (figure 6a) is lower than that shown in figure 4. The maximum 13.66 reached at $\gamma_2 = 135^\circ, \gamma_4 = 45^\circ$ and $\gamma_1 = \gamma_3 = 90^\circ$ (figure 6b) is equal to that shown in figure 4. This implies that the non-uniformity of the two side contact angles can help to reduce the minimum of B_c but never influence the maximum. Furthermore, the minimum of B_c attained by optimizing the non-uniform contact angles is far lower than the minima attained by changing the uniform contact angles and by increasing the aspect ratio to a very large value (Manning & Collicott 2015). Optimization of the non-uniform contact angles can therefore be considered as a more effective method of preventing the existence of liquid plugs.

3.3. Effect of aspect ratios for non-uniform contact angles

The aspect ratio of the tube with rectangular cross-section has been found to change the minimum of B_c but not to change the maximum 8.0, for uniform contact angles. Moreover, a very large aspect ratio ($= 100$) leads to a smaller value of B_c for uniform contact angles

Plugs in horizontal tubes with non-uniform contact angles

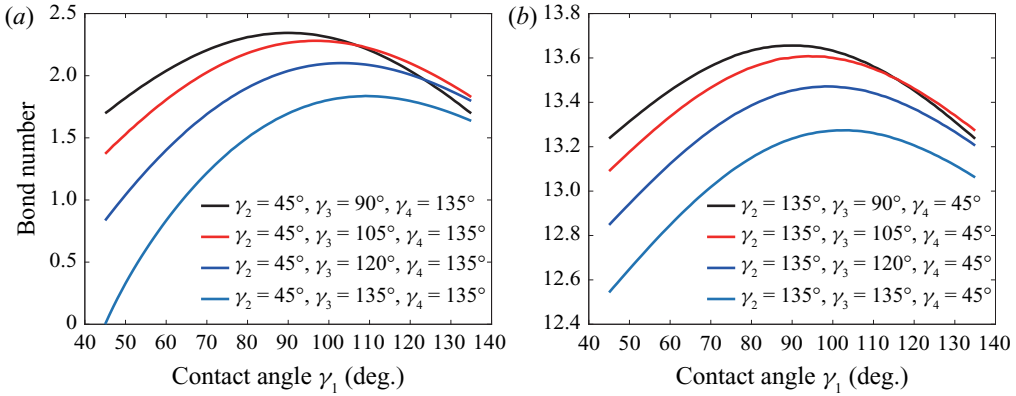


FIGURE 6. Critical Bond number of a square tube versus contact angle γ_1 with γ_3 changing among 90° , 105° , 120° and 135° for (a) $\gamma_2 = 45^\circ$ and $\gamma_4 = 135^\circ$ and (b) $\gamma_2 = 135^\circ$ and $\gamma_4 = 45^\circ$.

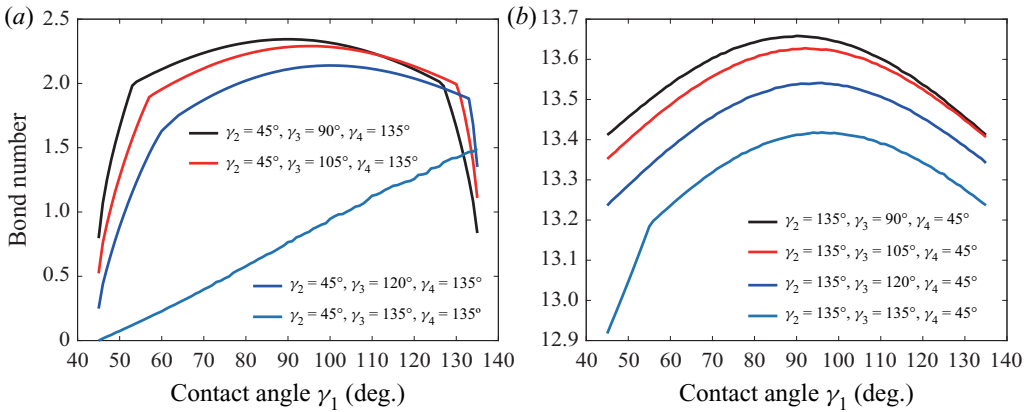


FIGURE 7. Critical Bond number of a rectangular tube ($w/h = 2$) versus contact angle γ_1 with γ_3 changing among 90° , 105° , 120° and 135° for (a) $\gamma_2 = 45^\circ$ and $\gamma_4 = 135^\circ$ and (b) $\gamma_2 = 135^\circ$ and $\gamma_4 = 45^\circ$.

	$w/h = 1$	$w/h = 2$	Contact angle conditions
Maximum	13.66	13.66	$\gamma_2 = 135^\circ$, $\gamma_4 = 45^\circ$ and $\gamma_1 = \gamma_3 = 90^\circ$
Minimum	0	0	$\gamma_1 = \gamma_2 = 45^\circ$ and $\gamma_3 = \gamma_4 = 135^\circ$

TABLE 1. Maximum and minimum critical Bond numbers.

46° or 134° , but it is still larger than 3.5 (Manning & Collicott 2015). Here, we intend to examine the effect of the aspect ratio of the rectangular cross-section on the minimum and maximum of B_c for a tube with walls of differing contact angles. As demonstrated in previous sections, the variation of contact angles is complex for comprehensively studying the effect of the non-uniformity of contact angles. In this context, the cases of γ_1 changing from 45° to 135° for $\gamma_2 = 45^\circ$ and 135° , $\gamma_3 = 90^\circ$, 105° , 120° and 135° and $\gamma_4 = 135^\circ$ and 45° are chosen, which include the two cases corresponding, respectively, to the minimum and maximum of B_c (figure 7).

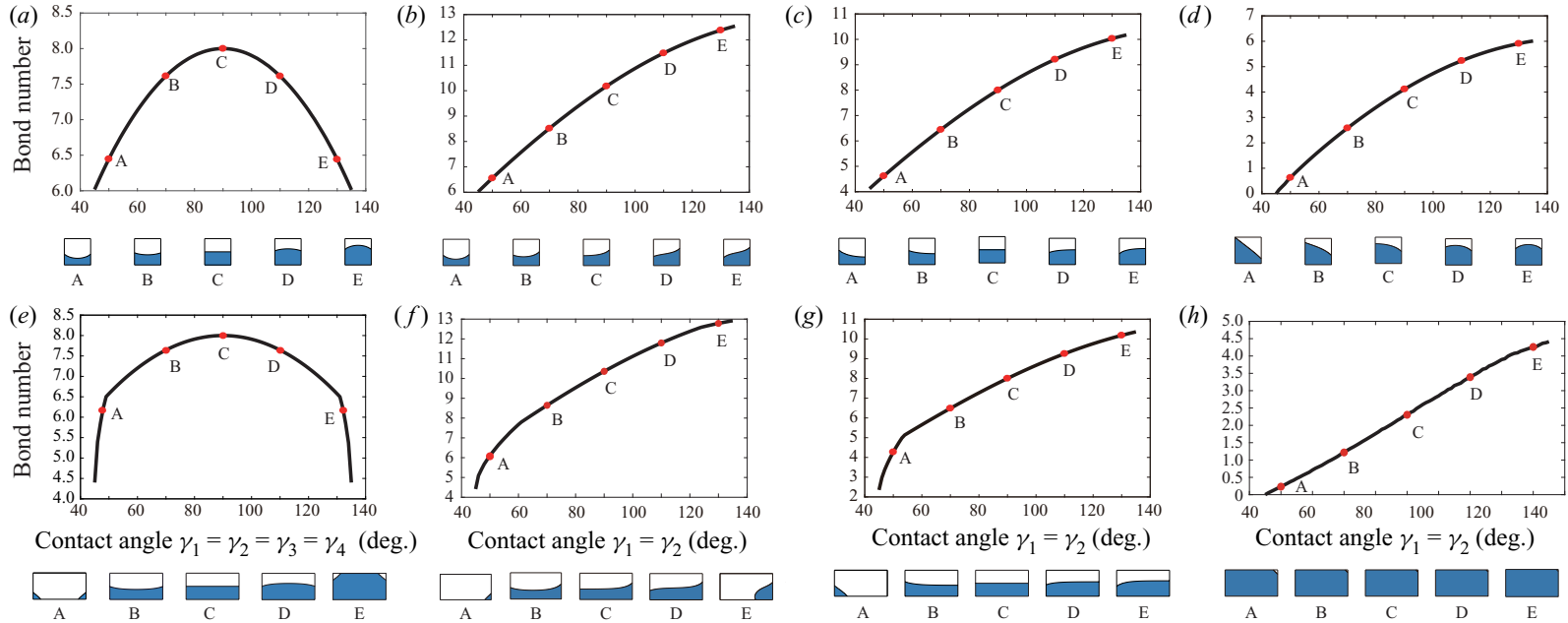


FIGURE 8. Critical Bond number as a function of contact angle for a capillary with two rectangular cross-sections: (a–d) square and (e–h) rectangle with $w/h = 2$. Panels (a) and (e) are for uniform contact angles, while panels (b–d) and (f–h) are for non-uniform contact angles. In the latter, the contact angles $\gamma_1 = \gamma_2$ vary from 45° to 135° and $\gamma_3 = \gamma_4 = 45^\circ$ (b and f), 90° (c and g) and 135° (d and h). The red circles denote the data at five representative contact angles, $\gamma_1 = \gamma_2 = 50^\circ, 70^\circ, 90^\circ, 110^\circ$ and 130° , which correspond to A, B, C, D and E, respectively. In order to have a clear mark on the curves, every red circle is so large that it approximately covers the three neighbouring points on a curve (e.g. the E red circle approximately covers the three points corresponding to $\gamma_1 = \gamma_2 = 129^\circ, 130^\circ$ and 131° , respectively).

Plugs in horizontal tubes with non-uniform contact angles

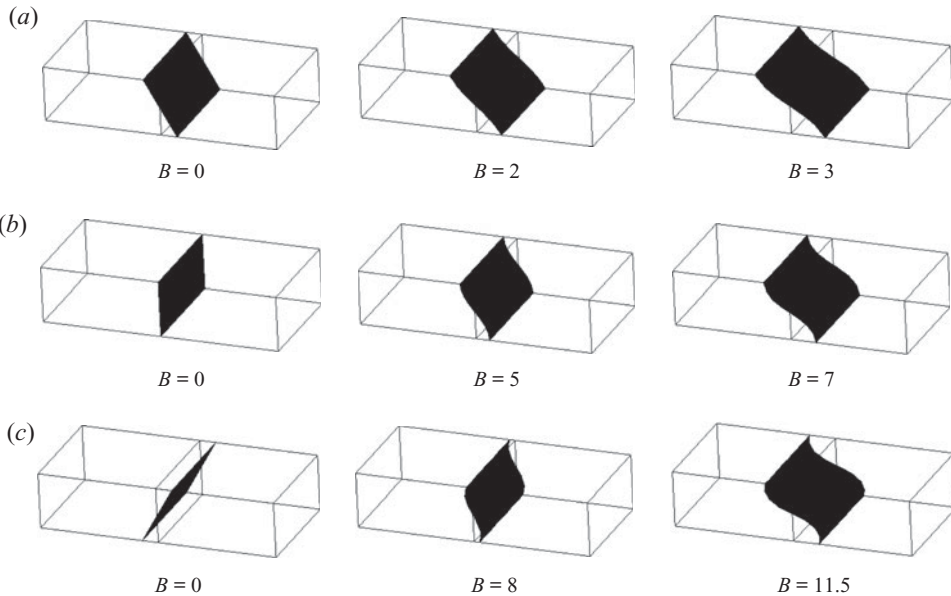


FIGURE 9. A three-dimensional view of the interface shapes for occluding liquid configurations in a rectangular tube ($w/h = 2$) for different cases directly calculated using Surface Evolver: (a) $\gamma_1 = 90^\circ$, $\gamma_2 = 60^\circ$, $\gamma_3 = 90^\circ$, $\gamma_4 = 120^\circ$; (b) $\gamma_1 = 90^\circ$, $\gamma_2 = 90^\circ$, $\gamma_3 = 90^\circ$, $\gamma_4 = 90^\circ$; and (c) $\gamma_1 = 90^\circ$, $\gamma_2 = 120^\circ$, $\gamma_3 = 90^\circ$, $\gamma_4 = 60^\circ$. The liquid and the gas are located at the left side and the right side of the interface shape in the tube, respectively. The critical Bond numbers for (a), (b) and (c) are 4.0, 8.0 and 12.0, respectively.

We compare the values of B_c for the chosen cases for a rectangle with $w/h = 2$ (figure 7) and a square (figure 6). It is found that the aspect ratio does not change the minimum and maximum of B_c (table 1). In other words, the aspect ratio of the rectangular cross-section has no effect on the minimum and maximum of B_c for a tube with walls of differing contact angles. This conclusion also can be obtained by substituting the contact angles for the minimum and maximum of B_c into (2.8) and (2.9). However, for the square, there is only one non-occluded liquid configuration with the gas–liquid interface meeting the two sidewalls (as the type 1 topology) while for the rectangle, besides the type 1 topology, another non-occluded liquid configuration having two contact points in one corner region or having four contact points in two separated corner regions may occur (as the type 2 topology) (figure 8). The transition between the two topologies is accompanied by the kink of the curve of B_c for the rectangle. Only one topology leads to no kink of the curve of B_c for the square. Figure 9 shows a three-dimensional view of the interface shapes for occluding liquid configurations in the rectangle with $w/h = 2$ for different cases directly calculated using Brakke’s Surface Evolver (1992).

4. Conclusions

In this paper, the existence of capillary plugs in liquid partially filling a horizontal rectangular tube with walls of differing contact angles in a downward gravity field is studied. The critical Bond numbers for a rectangular tube with walls of differing contact angles are analysed and the influence of the aspect ratio of the rectangular cross-section on the critical Bond number is examined. Compared to the cases for uniform contact angles, the maximum of B_c attained for $\gamma_2 = 135^\circ$, $\gamma_4 = 45^\circ$ and $\gamma_1 = \gamma_3 = 90^\circ$ is

greatly enhanced, and the minimum is significantly reduced to zero, which is reached for $\gamma_1 = \gamma_2 = 45^\circ$ and $\gamma_3 = \gamma_4 = 135^\circ$. The non-uniformity of contact angles can effectively make the formation of liquid plugs difficult in the tube. The aspect ratio of the rectangle has no effect on the minimum and maximum of B_c for the tube with walls of differing contact angles. There is only the type 1 topology in the square, while both type 1 topology and type 2 topology may occur in the rectangle with $w/h = 2$, and the transition between the two topologies is accompanied by the occurrence of a kink of the B_c curve. It is hoped that this paper will lay a solid foundation for the design of non-occluding tubes in a transverse body force field.

Acknowledgements

This research was supported in part by the National Natural Science Foundation of China (no. 11972170).

Declaration of interests

The authors report no conflict of interest.

References

- BHATNAGAR, R. & FINN, R. 2016 On the capillarity equation in two dimensions. *J. Math. Fluid Mech.* **18**, 731–738.
- BRÄKKE, K. A. 1992 The surface evolver. *Exp. Maths* **1**, 141–165.
- CHEN, Y. & COLLICOTT, S. H. 2006 Study of wetting in an asymmetrical vane–wall gap in propellant tanks. *AIAA J.* **44**, 859–867.
- CONCUS, P. & FINN, R. 1969 On the behavior of a capillary surface in a wedge. *Proc. Natl Acad. Sci.* **63**, 292–299.
- DE LAZZER, A., LANGBEIN, D., DREYER, M. & RATH, H. J. 1996 Mean curvature of liquid surfaces in cylindrical containers of arbitrary cross-section. *Microgravity Sci. Technol.* **9**, 208–219.
- DE LAZZER, A., STANGE, M., DREYER, M. & RATH, H. 2003 Influence of lateral acceleration on capillary interfaces between parallel plates. *Microgravity Sci. Technol.* **14**, 3–20.
- FINN, R. 1986 *Equilibrium Capillary Surfaces*. Springer.
- GRAVESEN, P., BRANEBJERG, J. & JENSEN, O. S. 1993 Microfluidics – a review. *J. Micromech. Microengng* **3**, 168–182.
- HERESCU, A. & ALLEN, J. S. 2012 The influence of channel wettability and geometry on water plug formation and drop location in a proton exchange membrane fuel cell flow field. *J. Power Sources* **216**, 337–344.
- MANNING, R. E. & COLLICOTT, S. H. 2015 Existence of static capillary plugs in horizontal rectangular cylinders. *Microfluid Nanofluid* **19**, 1159–1168.
- MANNING, R., COLLICOTT, S. & FINN, R. 2011 Occlusion criteria in tubes under transverse body forces. *J. Fluid Mech.* **682**, 397–414.
- POUR, N. B. & THIESSEN, D. B. 2019 Equilibrium configurations of drops or bubbles in an eccentric annulus. *J. Fluid Mech.* **863**, 364–385.
- RASCÓN, C., PARRY, A. O. & AARTS, D. G. A. L. 2016 Geometry-induced capillary emptying. *Proc. Natl. Acad. Sci.* **113**, 12633–12636.
- SMEDLEY, G. 1990 Containments for liquids at zero gravity. *Microgravity Sci. Technol.* **3**, 13–23.
- ZHANG, F. Y., YANG, X. G. & WANG, C. Y. 2006 Liquid water removal from a polymer electrolyte fuel cell. *J. Electrochem. Soc.* **153**, A225–A232.
- ZHOU, X. & ZHANG, F. 2017 Bifurcation of a partially immersed plate between two parallel plates. *J. Fluid Mech.* **817**, 122–137.